THE EFFECT OF Cr INTERLAYER ON THE CRYSTAL STRUCTURE AND CORROSION RESISTANCE OF CrN COATING ON STEEL

Dinh Thi Mong Cam, Nguyen Thanh Phuong, Nguyen The Quyen, Nguyen Huu Chi, Le Khac Binh, Tran Tuan, Duong Ai Phuong, Nguyen Chi Lang
University of Sciences, VNU-HCM

Abstract. *In this study, chromium nitride (CrN) hard coatings on stainless steel substrates with chromium (Cr) interlayers incorporated between the coatings and the steel substrates in order to improve adhesion of the coatings are investigated. Cr layers are prepared using d.c magnetron sputtering, and then CrN coatings are prepared using reactive d.c magnetron sputtering on these Cr layers. The effect of the Cr layer on the crystal structure and corrosion resistance of the CrN coating through surface modification is determined. The results show that regardless of whether the coatings include the Cr layers, face centered cubic structure of CrN phase with the preferred orientation on (111) planes parallel to coating surface remains and grain size of the CrN does not change. Nevertheless, the Cr layer induces stronger the (111) peak, reduces the residual stress and increases corrosion resistance of the CrN coatings. In addition, corrosion resistance of CrN coatings with the Cr layers deposited at different substrate bias and deposition time is similar although (111) peak intensity and residual stress of them change. The crystal structure and protection ability of the CrN/Cr coatings are optimum for Cr layers deposited with substrate bias of -60V and deposition time below 10min.*

Keywords: *Chromium nitride coatings, CrN/Cr coatings, CrN coatings, reactive d.c magnetron sputtering.*

1. INTRODUCTION

In recent years, the CrN coating has been identified as one of the most promising protective layers on surfaces of tools and dies thanks to its excellent mechanical properties and corrosion resistance. Nevertheless, the coatings deposited by physical vapor deposition sometimes exhibit poor adhesion because of the high internal stress [1]. The residual stress is generated in the coating due to the lattice mismatch between crystalline planes and the mismatch of the thermal contraction between the coating and the substrate [2]. The residual stress influences the mechanical properties of coated material. Besides, in aggressive environments, the major corrosion problem of the coated material is the defects in the coating, e.g. porosity, cracks, pinholes that are formed during the deposition process. These defects may form direct paths between the substrate and the exposed environment [3]. The application of a metallic intermediate layer between the substrate and coating helps to improve the adhesion, reduce the residual stress, limit the effect of the defects and increase the corrosion resistance of the substrate. Chen, Han, Chang et al [1-3, 6-7] have used a Cr interlayer to increase the corrosion and tribological resistance of the CrN coating. Electroplating technique is the conventional way of producing the Cr layers. However, the electroplating process adversely impacts the environment. Thus, sputter deposition is considered as an appropriate method to produce environmentally safe Cr layers.

The objective of this study is to investigate the effect of sputter-deposited Cr interlayers on the crystal structure and corrosion resistance of CrN coatings. Two sets of specimens are prepared: one has the Cr layer prepared by sputter deposition between the CrN film and the

substrate, denoted CrN/Cr and the other has the CrN layer directly deposited on the substrate, denoted CrN. The corrosion resistance of CrN/Cr is compared with that of CrN and bare steel by electrochemical method.

2. EXPERIMENTAL

2.1 Coating deposition

AISI 304 stainless steel (18% Cr, 9.0% Ni, 2.6% C, 70.4% Fe) was used as substrate in this study. The steel sheets of 1 mm of thicness were cut to an appropriate size of 20 mm x 30 mm. Prior to the deposition process, the steel substrates were ultrasonically cleaned in 3 chemical solutions: sodium hydroxide, chromic anhydride and aceton, and the substrate were then cleaned by Ar plasma at a high substrate bias of 500V for 30 mins.

The deposition was carried out using a 99.98% pure Cr target. The sputtering gas is a mixture of 99.999% pure Ar and 99.998% pure N_2 gases. The target-to-substrate distance was held constantly at 45 mm. During each experiment, the Cr target was first pre-sputtered under a 3 mtorr argon pressure at a deposition current of 1 A for 20 to 30 mins to remove any possible oxide layer. Immediately following the pre-sputtering process, the Cr interlayers were deposited by sputter deposition with different substrate bias and deposition time. Deposition pressure and current of Cr layers were kept constantly at 3 mtorr and 0.5A, respectively. The CrN coatings are then deposited by reactive d.c. magnetron sputtering for 60 mins. All CrN coatings in this study are deposited under a total Ar + N_2 gas pressure of 7.5 mtorr (N_2/Ar = 3/2) with a substrate bias of -50 V and a deposition current of 1 A. These optimal deposition conditions of the CrN coating were determined in our previous studies [4, 5]. The deposition conditions and some of properties of the coatings are summarized in Table 1.

Table 1. Deposition conditions for coatings, grain size (D), residual stress (σ_f), and corrosion potential (E_{corr}) of specimens obtained

Sample	Substrate bias [V]	Deposition time [min]	Preferred orientation	D [nm]	σ_f [GPa]	E_{corr} [V]
Steel	-	-	-	-	-	0.58
CrN	-50	60	CrN(111)	33.38	-22.97	0.86
CrN/Cr -19	-50/-25	60/30	CrN(111)	32.05	-17.00	0.97
CrN/Cr -20	-50/-50	60/30	CrN(111)	33.76	-17.60	0.95
CrN/Cr -21	-50/-60	60/30	CrN(111)	35.94	-14.62	0.96
CrN/Cr -22	-50/-80	60/30	CrN(111)	33.63	-14.92	0.95
CrN/Cr-24	-50/-50	60/20	CrN(111)	36.34	-19.10	0.97
CrN/Cr-25	-50/-50	60/10	CrN(111)	35.35	-18.20	0.98
CrN/Cr-27	-50/-25	60/10	CrN(111)	32.85	-19.69	0.97
CrN/Cr-28	-50/-25	60/20	CrN(111)	34.37	-21.18	0.97

2.2 Coating characterization

The phase and structure of CrN coatings with and without Cr layers were analyzed by X-ray diffraction (XRD) with CuK_α radiation (λ = 0.154 nm). The specimens are investigated using $\theta/2\theta$ diffraction mode ranging from 20° to 60°. The crystal structure of the coatings is determined by comparing their angles and intensities of diffraction peaks with those reported

from Joint Committee of Powder Diffraction Standards (JCPDS). Form XRD spectra, the residual stresses (σ_f) of coatings were calculated using the Stoney's equation:

$$\sigma_f = -\frac{E(d - d_o)}{2\upsilon d_o} \quad (1)$$

where υ (0.28) is the Poisson's ratio; E (400 GPa for (111) CrN) was Young's modulus; d_o (2.394 A° for the (111) planes) is the stress free lattice spacing; d is the strained lattice spacing of the coating.

The corrosion behavior of CrN coatings with and without Cr layers is investigated by cyclic polarization (CP) method. This electrochemical technique is an accelerated method for determining the characteristic corrosion potential E_{corr}. E_{corr} is evaluated by the cyclic polarization curves (current-potential curves) over a small potential range from - 0.5 V/sce to 1 V/sce. Electrochemical measurements were carried out in a standard three-electrode cell with a saturated calomel reference electrode (sce). AISI 304 stainless steel, CrN and CrN/Cr specimens are immersed in an aerated 3.5 % NaCl solution for corrosion tests.

3. RESULTS AND DISCUSSION

3.1 Crystal structure and residual stress of coatings

As mentioned earlier, CrN exists in different phases so there is a limited range of nitrogen concentration wherein stoichiometric phase of CrN with B1 structure (face centered cubic) exists. Therefore it is essential to optimize the process parameters for the deposition of stoichiometric cubic CrN phases. The optimal deposition conditions were determined in our previous study [4, 5] and under these conditions, (111) preferred orientation cubic phase of CrN was obtained (Fig. 1). After optimizing the deposition conditions for CrN coating, CrN/Cr samples were prepared under different deposition conditions of Cr layers.

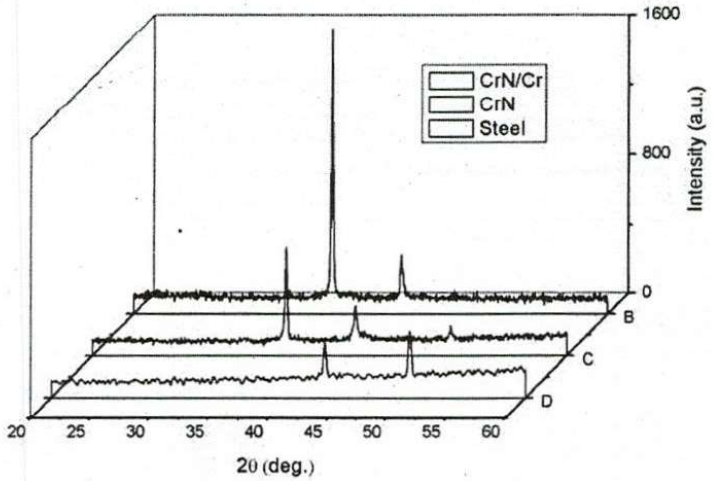

Fig. 1. XRD patterns of steel, CrN and CrN/Cr specimens.

The XRD spectra of CrN coatings with and without a Cr interlayer (Fig. 1) are consistent with the JCPDS database of CrN phase. Both cases have the same preferred orientation of CrN (111). However, a Cr layer incorporated between the CrN coating and the substrate drastically increases (111) peak intensity of the CrN coating.

The full width at half maximum (FWHM) of the diffraction peak represents the grain size in Scherrer's equation. The FWHMs of the (111) peaks for CrN and CrN/Cr specimens vary slightly from 0.23^0 to 0.26^0 so that grain sizes of the CrN coatings in both cases are similar.

The Cr interlayer does not affect the preferred orientation and grain size of the CrN coatings; this fact is consistent with the authors' previous studies on Cr interlayer deposited by electroplating and MEVVA (metal vapor vacuum arc) [6,7].

The residual stresses of the CrN and CrN/Cr specimens are evaluated and compared. Residual stresses often exist in deposition coatings and originate from two major sources: one is the intrinsic stress that depends on deposition parameters such as ion bombardment energy, and the other is the thermal stress caused by the different thermal expansion coefficients between the coating and the substrate. Therefore, the residual stress is mainly the intrinsic stress in this case. As shown in the Fig. 1, the (111) diffracted peaks of CrN coatings with Cr layers shift towards higher angles, indicating the lower residual stress in the coatings. The residual stresses are calculated experimentally using Eq. (1) for the (111) planes. The calculating results are listed in Table 1. To our surprise, Cr interlayer drastically reduces the residual stress in the CrN coating. The reduction of stress $\Delta\sigma$ can be defined as:

$$\Delta\sigma = \left|\left(\sigma_{CrN/Cr} - \sigma_{CrN}\right)/\sigma_{CrN}\right| \times 100\% \qquad (2)$$

where $\sigma_{CrN/Cr}$ and σ_{Cr} are the corresponding residual stress with and without the Cr interlayer, respectively.

The above results demonstrate that the role of the Cr interlayer is apparent: this layer significantly reduces the residual stress of the CrN coating by up to 36.4%, but it does not affect the preferred orientation and the grain size of the CrN coating.

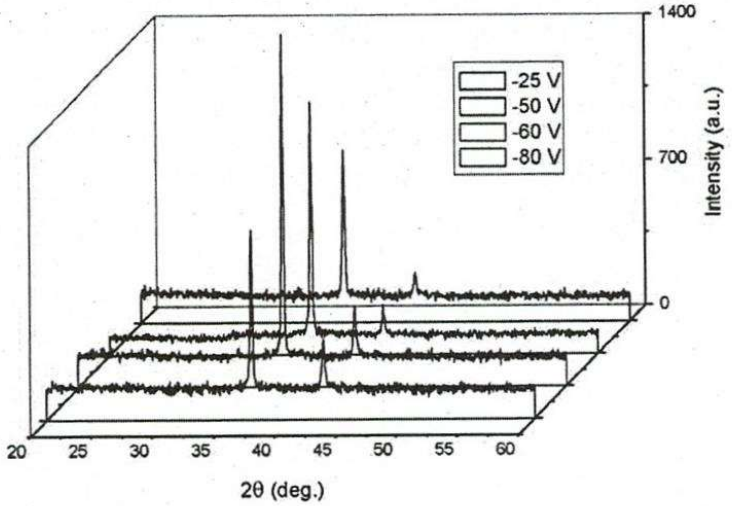

Fig. 2. XRD patterns of CrN/Cr-19 (V_b = -25V), CrN/Cr-20 (V_b = -50V), CrN/Cr-21 (V_b = -60V), CrN/Cr-22 (V_b = -80V)

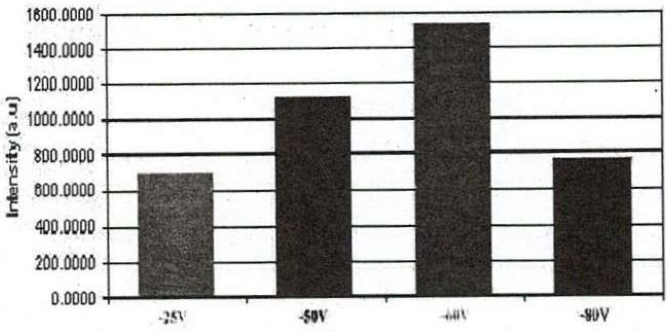

Fig. 3. Substrate bias effects on (111) CrN diffraction intensity of CrN/Cr specimens

XRD spectra of the CrN coatings with Cr layers deposited for various substrate bias of -25, -50, -60, and -80 V are compared in order to understand more distinctly the effects of Cr layers on the crystal structure of CrN coatings. As shown in Fig. 2, the diffraction patterns of specimens reveal the presence of CrN cubic phase, and the (111) preferred orientation for the CrN coatings with the different Cr layers. However, when the substrate bias is increased from -25 to -60 V, the intensity of (111) diffraction peaks significantly increases (Fig. 3) and position of the peaks is slightly shifted to higher 2θ values indicating a reduction in residual stress (Fig. 4). At higher substrate bias ($V_b \geq$ -80 V), the intensity (111) peaks decrease. When the substrate bias is below -60 V, energy and density of the impinging ions bombarded on growing Cr layer increase, and a better crystallized Cr layer is then obtained, the structure of CrN coating grown on this Cr layer is also better. But as the energy of the impinging ions increases more strongly ($V_b \geq$ -80 V), re-sputtering occurs and generation of defects in the Cr layer increases, thus (111) peak intensity of the CrN coating grown on this Cr layer decreases. Furthermore, reduction of residual stress of the CrN coatings can be explained by ion bombardment during the coating growth. The Cr interlayers deposited under different substrate biases affect the (111) peak intensity and the residual stress but do not affect the preferred orientation of the coatings.

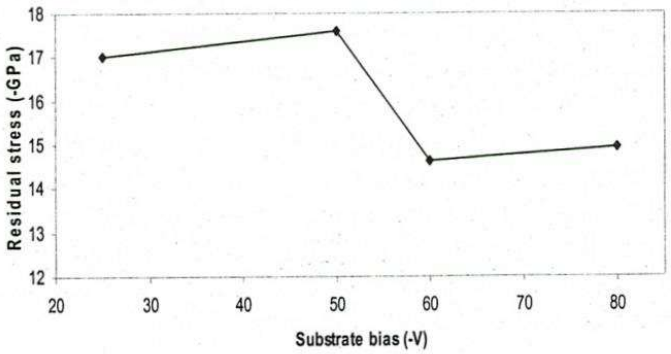

Fig. 4. Residual stress of CrN coatings as a function of substrate bias

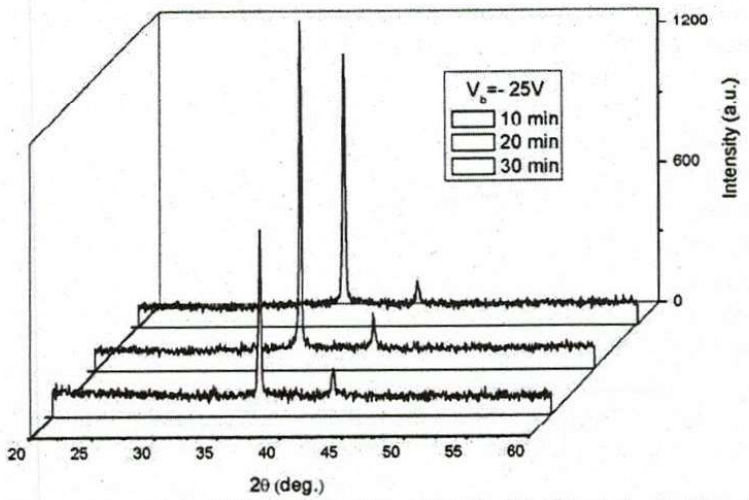

Fig. 5. XRD patterns of CrN/Cr-27 (10min), CrN/Cr-28 (20min), CrN/Cr-19 (30min)

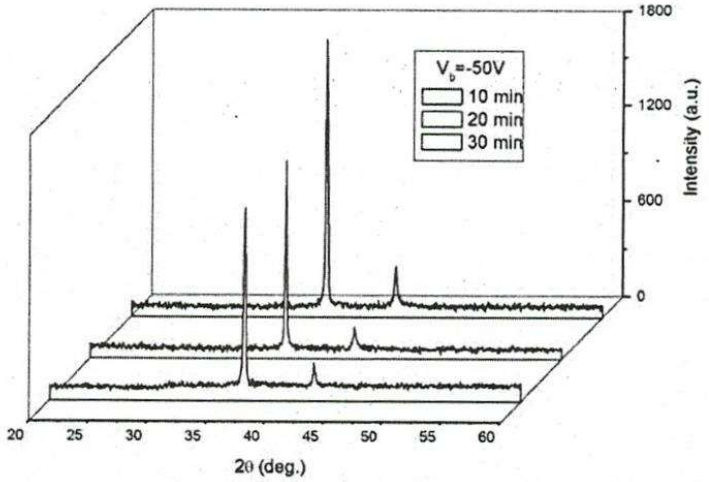

Fig. 6. XRD patterns of CrN/Cr-25 (10min), CrN/Cr-24 (20min), CrN/Cr-20 (30min)

Also, similar phenomenons are observed with the variation of deposition time of Cr interlayers. The XRD spectra of the CrN coatings with different deposition time of Cr layers (10, 20 and 30 min) at substrate biases of -25V (Fig. 5) and -50V (Fig. 6) show that deposition time of Cr layers does not vary the (111) preferred orientation of CrN coatings. The intensity of this (111) peak is maximum when deposition time is 20 minutes in the case of V_b = -25V, and 10 minutes when V_b = -50V. Thus there is a certain value of thickness of Cr layer that lead to the formation of the best crystal structure of CrN coating. As mentioned above, this value of Cr layer can be found at the deposition time of 20 minutes at V_b = -25V and 10 min at V_b = -50V. The energy and density of the impinging ions bombarded on the growing Cr layer increase proportionally to the substrate bias. So the higher substrate bias is, the sooner the Cr layers reach this ideal thickness. It may be concluded that the thickness of the Cr interlayer also influences the crystal structure of the CrN coating.

3.2 Electrochemical behavior

The corrosion resistance of CrN/Cr is compared with that of CrN and bare steel. The polarization curves of potential (relative to sce) vs. current density are shown in Fig. 7 and Fig. 8. Corrosion potentials of specimens are listed in Table 1.

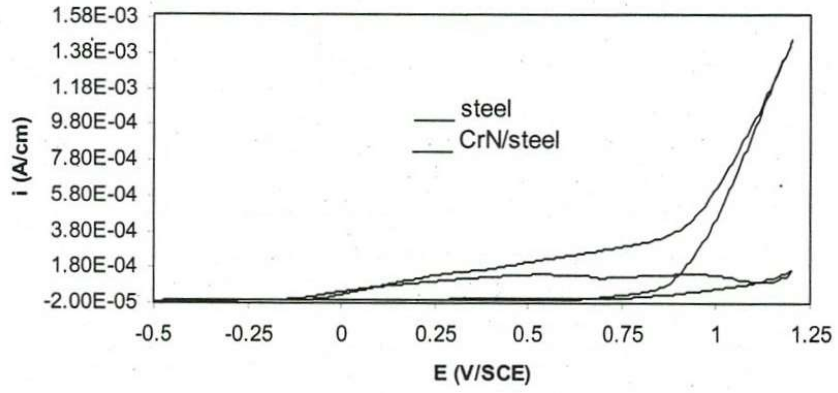

Fig. 7. Polarisation curves of steel and CrN/steel in 3.5%NaCl solution

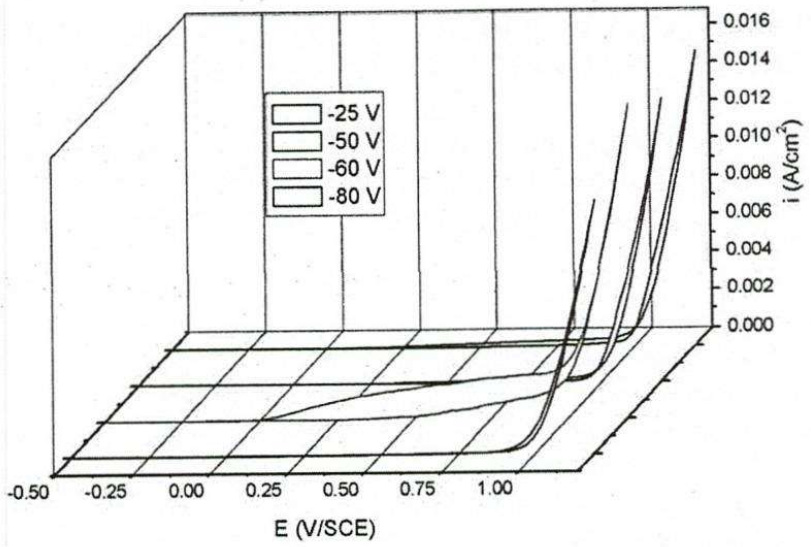

Fig. 8. Polarisation curves of CrN/Cr-19 (-25V), CrN/Cr- 20 (-50V), CrN/Cr-21 (-60V), CrN/Cr- 22 (-80V)

The E_{corr} value of CrN (0.86V/sce) is significantly higher than that of bare steel (0.58V/sce), indicating that the CrN coating deposited steel surface improves the corrosion resistance. The E_{corr} of CrN specimen decreases more than that of CrN/Cr specimen (~ 0.98V/sce), showing that CrN/Cr possesses a better capability of preventing the localized galvanic attack between the coating and the substrate. The performance of the coated steels against corrosion is strongly affected by defects of the coating [3]. The Cr layer promotes the surface passivity of the steel substrate and isolates physically the structure defects of the CrN coatings. It may be concluded from these observations that the Cr layer in CrN/Cr/steel provides a beneficial effect on the corrosion resistance of the steel.

Fig. 8 shows polarization curves of CrN/Cr specimens with Cr interlayers deposited for various substrate bias of -25, -50, -60, and -80 V. The polarization curves and E_{corr} values of specimens indicate that despite diffirent Cr interlayers, the corrosion resistance of all CrN/Cr/steel specimens is similar. The Cr interlayer effectively reduces the corrosion, but this corrosion resistance does not change when altering the Cr interlayer. Thus electrochemical behavior of coated steel seems to be controled by the outer layer.

4. CONCLUSIONS

In this study, CrN coatings with and without the Cr interlayers are successfully synthesized using d.c. magnetron sputtering (for Cr layers) and reactive d.c. magnetron sputtering (for CrN layers). the CrN coatings have only CrN cubic phase with (111) preferred orientation in both case without and with the different Cr interlayers. Although the Cr interlayer does not affect the grain size of CrN, it significantly reduces the residual stress of the CrN coating by up to 36.4 % and increases the corrosion resistance of the CrN coating. When increasing the substrate bias of the Cr interlayers from -25 V to -60 V, the crystal structures of the CrN coatings are better, the residual stresses of the CrN coatings decrease but the corrosion resistance does not change. The higher substrate bias of Cr interlayer is, the sooner Cr interlayer reach the ideal thickness which induces the best crystal structure of CrN coating.

ẢNH HƯỞNG CỦA LỚP ĐỆM Cr LÊN CẤU TRÚC TINH THỂ VÀ ĐỘ CHỐNG ĂN MÒN CỦA MÀNG CrN PHỦ TRÊN ĐẾ INOX

Đinh Thị Mộng Cầm, Nguyễn Thanh Phương, Nguyễn Thế Quyền, Nguyễn Hữu Chí, Lê Khắc Bình, Trần Tuấn, Dương Ái Phương, Nguyễn Chi Lăng
Trường Đại học Khoa học Tự nhiên, ĐHQG-HCM

Tóm tắt: *Trong các nghiên cứu trước, chúng tôi đã chế tạo thành công màng CrN phủ trực tiếp trên đế inox. Màng tạo ra có độ cứng cao và có ứng dụng cụ thể trong thực tế. Tuy nhiên độ bám dính của màng trên đế inox cần được cải thiện. Trong báo cáo này, chúng tôi tiến hành tổng hợp màng cứng CrN trên đế inox có lớp đệm Cr để gia tăng độ bám dính của màng. Màng CrN và lớp đệm Cr đều được tạo bằng phương pháp phún xạ magnetron và lớp Cr được phủ tại nhiều điều kiện khác nhau để khảo sát sự ảnh hưởng của nó lên cấu trúc và độ chống ăn mòn của màng CrN. Kết quả khảo sát cho thấy màng CrN phủ trực tiếp trên đế inox và phủ trên lớp inox có lớp đệm Cr đều xuất hiện một pha duy nhất thuộc cấu trúc lập phương tâm mặt với định hướng ưu tiên theo mặt (111) song song với bề mặt màng và kích thước hạt của CrN trong hai trường hợp không thay đổi. Tuy nhiên, nếu màng CrN phủ trên inox có lớp Cr ở giữa thì cường độ đỉnh phổ (111) tăng lên đáng kể, ứng suất nén của màng CrN giảm đến 36.4% và độ chống ăn mòn của màng tăng. Hơn nữa, có sự thay đổi cường độ đỉnh (111) và ứng suất của màng CrN khi phủ trên lớp Cr được tạo ở các thế hiệu dịch và thời gian khác nhau, mặc dù độ chống ăn mòn của các màng CrN thì tương tự nhau. Khi lớp Cr được tạo với thời gian dưới 10 phút và thế hiệu dịch -60V thì màng CrN/Cr có cấu trúc tinh thể và khả năng bảo vệ tốt nhất.*

Từ khóa: *Màng cứng CrN, màng CrN/Cr, phún xạ phản ứng magnetron d.c.*

REFERENCES

[1]. Hong-Ying Chen, Sheng Han, Han C. Shih, Materials Letters, 58, 2924 (2004).
[2]. S. Han, H.Y. Chen, Z.C. Chang, K.W. Weng, D.Y. Wang, F.H. Lu, H.C. Shih, Thin Solid Films, 447-448, 425 (2004).
[3]. K.L. Chang, S. Han, J.H. Lin, J.W. Hus, H.C. Shih, Surf. Coat. Technol., 172, 72–78 (2003).
[4]. Dinh Thi Mong Cam, Master of Science Thesis, 2008.
[5]. Dinh Thi Mong Cam, Nguyen Huu Chi, Le Khac Binh, Tran Tuan, Nguyen Thi Hai Yen, Tran Quang Trung, Science & Technology Development, Vol. 10, 5 (2007).
[6]. S. Han, J.H. Lin, X.J. Guo, S.H. Tsai, Y.O. Su, J.H. Huang, F.H. Lu, H.C. Shih, Thin Solid Films, 377-378, 578 (2000).
[7]. S. Han, H.Y. Chen, Z.C. Chang, J.H. Lin, C.J. Yang, F.H. Lu, F.S. Shieu, H.C. Shih, Thin Solid Films, 436, 238 (2003).